

# 1 **Estimation of sulfuric acid concentration using ambient ion** 2 **composition and concentration data obtained by Atmospheric** 3 **Pressure interface Time-of-Flight ion mass spectrometer**

4 Lisa J. Beck<sup>1</sup>, Siegfried Schobesberger<sup>2</sup>, Mikko Sipilä<sup>1</sup>, Veli-Matti Kerminen<sup>1,4</sup> and Markku  
5 Kulmala<sup>1,3,4,5</sup>

6 <sup>1</sup>Institute for Atmospheric and Earth System Research/Physics, University of Helsinki, 00014 Helsinki, Finland

7 <sup>2</sup>Department of Applied Physics, University of Eastern Finland, 70211 Kuopio, Finland

8 <sup>3</sup>Aerosol and Haze Laboratory, Beijing Advanced Innovation Center for Soft Matter Sciences and Engineering,  
9 Beijing University of Chemical Technology (BUCT), Beijing, China

10 <sup>4</sup>Joint International Research Laboratory of Atmospheric and Earth System Sciences, School of Atmospheric  
11 Sciences, Nanjing University, Nanjing, China

12 <sup>5</sup>Faculty of Geography, Lomonosov Moscow State University, Moscow, Russia

13  
14 *Correspondence to:* Lisa Beck (lisa.beck@helsinki.fi) and Markku Kulmala (markku.kulmala@helsinki.fi)

## 15 **Abstract**

16 Sulfuric acid (H<sub>2</sub>SO<sub>4</sub>, SA) is the key compound in atmospheric new particle formation. Therefore, it is crucial to  
17 observe its concentration with sensitive instrumentation, such as chemical ionisation (CI) inlets coupled to  
18 Atmospheric Pressure interface Time-of-Flight mass spectrometers (APi-TOF). However, there are environmental  
19 conditions and physical reasons when chemical ionisation cannot be used, for example in certain remote places  
20 or flight measurements with limitations regarding chemicals. Here, we propose a theoretical method to estimate  
21 the SA concentration based on ambient ion composition and concentration measurements that are achieved by  
22 APi-TOF alone. We derive a theoretical expression to estimate SA concentration and validate it with accurate CI-  
23 APi-TOF observations. Our validation shows that the developed estimate works well during daytime in the boreal  
24 forest ( $R^2 = 0.85$ ), however it underestimates the SA concentration in e.g. Antarctic atmosphere during new  
25 particle formation events where the dominating pathway for nucleation involves sulfuric acid and a base ( $R^2 =$   
26  $0.48$ ).  
27  
28  
29

## 30 **1 Introduction**

31 Sulfuric acid (H<sub>2</sub>SO<sub>4</sub>, SA) is the key compound in atmospheric new particle formation (e.g. Weber et al., 1995,  
32 1996; Birmili et al., 2003; Kulmala et al., 2004; Kuang et al., 2008; Kerminen et al., 2010; Wang et al., 2011;  
33 Kulmala et al., 2014; Yao et al., 2018; Cai et al., 2021), therefore it is crucial to have accurate observations of its  
34 concentration. However, ambient concentrations of H<sub>2</sub>SO<sub>4</sub> are low, commonly less than a part per trillion by  
35 volume ( $\sim 2 \cdot 10^7$  molecules cm<sup>-3</sup>), making it challenging to measure it. During the recent years there have been  
36 instrumental developments towards a reliable detection of H<sub>2</sub>SO<sub>4</sub> in the atmosphere, particularly via the  
37 development of a Chemical Ionisation Atmospheric Pressure interface Time-of-Flight mass spectrometer (CI-

38 APi-TOF, Jokinen et al., 2012), using nitric acid as a reagent ion. Still, the measurement technique with CI-APi-  
39 TOF is relatively challenging, as a thorough calibration i.e. with sulfuric acid as proposed by Kürten et al. (2012),  
40 is needed in order to get reliable numbers. Furthermore, the loss of sulfuric acid to surfaces, such as an inlet, and  
41 the correct flow rates must be known and characterised.

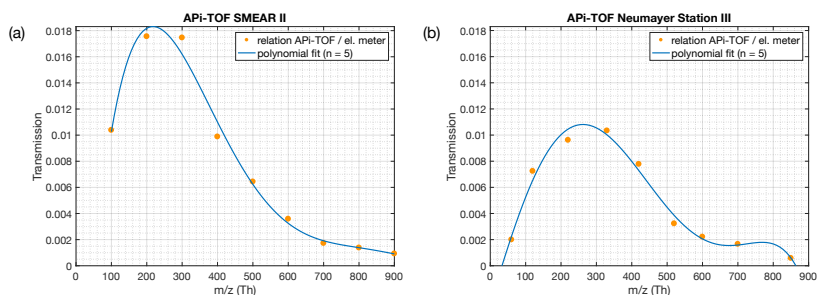
42  
43 During the past decade, Atmospheric Pressure interface Time-of-Flight mass spectrometers (APi-TOF, Junninen  
44 et al., 2010) have been deployed in several measurement campaigns where the use of a CI inlet was either not  
45 possible or desired. In these instances, the APi-TOF only observed the composition and concentration of ambient  
46 ions. The APi-TOF is capable of directly sampling and detecting naturally charged gas-phase ions, including  
47 molecular clusters, and is often being used to detect clustering processes as a first step of new particle formation  
48 on a molecular basis (e.g. Schobesberger et al., 2013; Jokinen et al., 2018; Beck et al., 2021). While a CI-APi-  
49 TOF at best has a limit of detection of around  $\sim 10^4$  molecules  $\text{cm}^{-3}$  ( $\sim$  ppq level), the APi-TOF can detect  
50 approximately 1% of the ambient ion concentration (Fig. 1, Junninen et al., 2010). With an average ion  
51 concentration of  $\sim 1000$   $\text{cm}^{-3}$  per polarity (Hirsikko et al., 2011), the APi-TOF is measuring 10 ions  $\text{cm}^{-3}\text{s}^{-1}$  with a  
52 limit of detection of  $\sim 0.01$  counts per second, hence 0.1 ions  $\text{cm}^{-3}$ . This corresponds to approximately a pps level  
53 ( $100 \cdot 10^{-21}$ ), showing that the limit of detection of an APi-TOF in comparison to a CI-APi-TOF is lower by five  
54 orders of magnitudes.

55  
56 A detailed description of the APi-TOF can be found in Junninen et al. (2010). Since concentrations of neutral  
57 clusters are below the detection limit of CI-APi-TOF in many atmospheric conditions and environments, using  
58 the APi-TOF is currently the only way to directly detect atmospheric clustering. Therefore, if we can estimate  
59  $\text{H}_2\text{SO}_4$  concentration particularly during initial steps of new particle formation, based on the same dataset, we can  
60 readily get better insight into the process itself.

61  
62 Since there are only limited long term observations of  $\text{H}_2\text{SO}_4$  concentrations, several proxies on this concentration  
63 have been developed (e.g. Petäjä et al., 2009; Mikkonen et al., 2011; Lu et al., 2019; Dada et al., 2020). These  
64 proxies attempt to approximate the ambient  $\text{H}_2\text{SO}_4$  concentrations using more readily measured quantities, in  
65 particular the sulfur dioxide concentration, (UV) radiation intensity and pre-existing particle number size  
66 distribution that can be used to calculate the condensation sink for gas-phase  $\text{H}_2\text{SO}_4$ . In circumstances where the  
67 required data for  $\text{H}_2\text{SO}_4$  proxies are not available, but measurements with an APi-TOF were conducted, the  $\text{H}_2\text{SO}_4$   
68 concentration can be obtained from the ion mass spectra. A first attempt of estimating the sulfuric acid  
69 concentration via the concentration of atmospheric ions was introduced by Arnold and Fabian (1980), followed  
70 by Eisele (1989) under the assumption that most  $\text{H}_2\text{SO}_4$  molecules are charged by reacting with  $\text{NO}_3^-$ .

71  
72 Motivated by the reasonings outlined above, we derive here an expression to estimate  $\text{H}_2\text{SO}_4$  concentration based  
73 primarily on APi-TOF observations and validate it.

74  
75  
76



77

78

79

80

81

82

83

84

85

## 2 Theoretical estimation of sulfuric acid concentration with bisulphate ion and H<sub>2</sub>SO<sub>4</sub> clusters

86

87

88

89

90

91

92

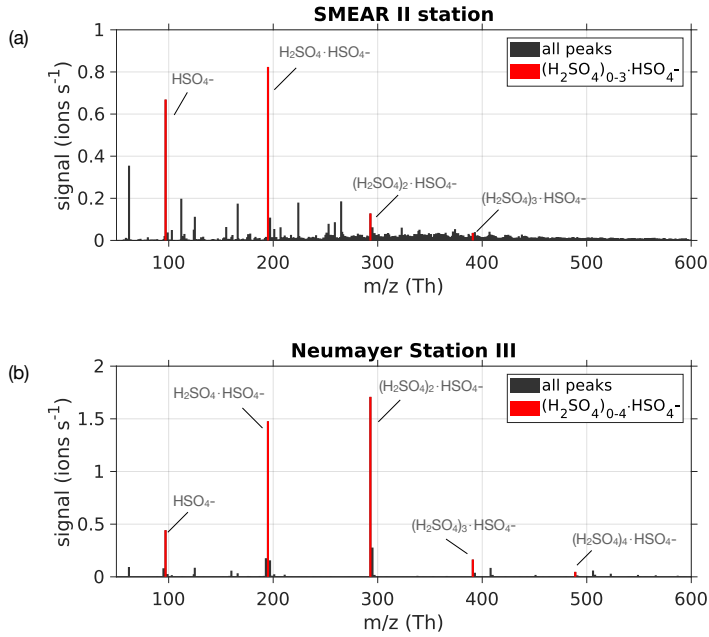
93

94

95

96

Ambient ion mass spectra have usually clear evidence of gas-phase H<sub>2</sub>SO<sub>4</sub>, predominantly in the form of bisulphate ion (HSO<sub>4</sub><sup>-</sup>) and its adducts involving H<sub>2</sub>SO<sub>4</sub>, forming so-called dimers (H<sub>2</sub>SO<sub>4</sub>·HSO<sub>4</sub><sup>-</sup>) as well as larger clusters (Ehn et al., 2010). These ions are due to the efficient scavenging of a negative charge by ambient H<sub>2</sub>SO<sub>4</sub> via proton donation, and due to the high stability of the sulfuric acid-bisulphate ion clusters, in particular for the dimer (Ortega et al., 2014). In order to estimate the sulfuric acid concentration (H<sub>2</sub>SO<sub>4</sub>) using measured naturally charged ions (see Fig. 2), we approximate this concentration by following the bisulphate ion HSO<sub>4</sub><sup>-</sup>, herein denoted SA<sub>monomer</sub>, the dimer cluster H<sub>2</sub>SO<sub>4</sub>·HSO<sub>4</sub><sup>-</sup> (SA<sub>dimer</sub>) and trimer cluster (H<sub>2</sub>SO<sub>4</sub>)<sub>2</sub>·HSO<sub>4</sub><sup>-</sup> (SA<sub>trimer</sub>). Any other H<sub>2</sub>SO<sub>4</sub>-containing ion clusters, in particular those larger than the SA<sub>trimer</sub>, typically occur at much smaller concentrations and will be neglected here.



97  
 98 **Figure 2** (a) Mass spectrum from 50 to 600 Th measured with the APi-TOF on 24 May 2017 during the time period 08:00 –  
 99 18:00 (local time) at SMEAR II station, Hyttiälä, Finland. (b) Mass spectrum from 14 January 2019 between 08:00 and 18:00  
 100 (local time) at Neumayer Station III, Antarctica during a new particle formation event. The bisulphate ion  $\text{HSO}_4^-$  and  $\text{H}_2\text{SO}_4$   
 101 clusters containing it were used for the estimation of  $\text{H}_2\text{SO}_4$  concentration, and are coloured in red.

102  
 103

104 If we assume that the concentration of  $\text{SA}_{\text{monomer}}$  depends generally on its production rate ( $P_1$ ) and that its loss is  
 105 by condensation onto aerosol particles (condensation sink, CS), to the  $\text{SA}_{\text{dimer}}$  when clustering with another  $\text{H}_2\text{SO}_4$   
 106 molecule, and to ion-ion recombination with positive ions ( $N_{\text{pos}}$ ), we get the following equation for the  $\text{SA}_{\text{monomer}}$   
 107 concentration:

108

$$\frac{d[\text{SA}_{\text{monomer}}]}{dt} = P_1 - \text{CS} \cdot [\text{SA}_{\text{monomer}}] - P_2 - \alpha \cdot [\text{SA}_{\text{monomer}}] \cdot N_{\text{pos}}, \quad (1)$$

109

110 where  $P_2 = k_1 \times [\text{SA}_{\text{monomer}}] \times [\text{H}_2\text{SO}_4]$  is the dimer production rate due to  $\text{SA}_{\text{monomer}}\text{-H}_2\text{SO}_4$  collisions,  $\alpha$  ( $\approx 1.6$   
 111  $\times 10^{-6} \text{ cm}^3 \text{ s}^{-1}$ ) is the ion-ion recombination coefficient (Kontkanen et al., 2013), and the collision rate  $k_1$  is assumed  
 112 to be constant.

113

114 For the dimer concentration we consider the production  $P_2$ , the loss due to CS, the clustering of the  $SA_{dimer}$  with  
 115  $H_2SO_4$  with a rate constant  $k_2$ , and the ion-ion recombination:  
 116

$$\frac{d[SA_{dimer}]}{dt} = P_2 - CS \cdot [SA_{dimer}] - k_2 \cdot [SA_{dimer}] \cdot [H_2SO_4] - \alpha \cdot [SA_{dimer}] \cdot N_{pos}, \quad (2)$$

117  
 118 And with substituting  $P_2$ , eq. 2 for  $SA_{dimer}$  changes to:  
 119

$$\frac{d[SA_{dimer}]}{dt} = k_1 \cdot [SA_{monomer}] \cdot [H_2SO_4] - CS \cdot [SA_{dimer}] - k_2 \cdot [SA_{dimer}] \cdot [H_2SO_4] - \alpha \cdot [SA_{dimer}] \cdot N_{pos}. \quad (3)$$

120  
 121 Finally, to produce  $SA_{trimer}$  we consider the collision of the  $SA_{dimer}$  with  $H_2SO_4$  and the loss to the CS and ion-ion  
 122 recombination. For the sake of completeness, we would additionally have to consider the loss of  $SA_{trimers}$  to form  
 123 the tetramer  $(H_2SO_4)_3 \cdot HSO_4$ , however this additional term is rather small and will therefore be neglected in this  
 124 derivation. Therefore, we get the simplified equation for  $SA_{trimer}$ :  
 125

$$\frac{d[SA_{trimer}]}{dt} = k_2 \cdot [SA_{dimer}] \cdot [H_2SO_4] - CS \cdot [SA_{trimer}] - \alpha \cdot [SA_{trimer}] \cdot N_{pos}. \quad (4)$$

126  
 127 For simplification, we consider a pseudo-steady state condition for both dimers and trimers by setting the left-  
 128 hand side of eqs. (3) and (4) to be zero, which is justified when the dimer and trimer concentrations change at  
 129 rates smaller than their overall production and loss rates. Thereby, from eq. (3) we obtain:  
 130

$$\begin{aligned} & k_1 \cdot [SA_{monomer}] \cdot [H_2SO_4] \\ & = CS \cdot [SA_{dimer}] + k_2 \cdot [SA_{dimer}] \cdot [H_2SO_4] + \alpha \cdot [SA_{dimer}] \cdot N_{pos} \end{aligned} \quad (5)$$

131  
 132 and from eq. (4) we obtain:  
 133

$$k_2 \cdot [SA_{dimer}] \cdot [H_2SO_4] = CS \cdot [SA_{trimer}] + \alpha \cdot [SA_{trimer}] \cdot N_{pos}. \quad (6)$$

134  
 135 If we now deploy equation (6) in equation (5) and solve for  $H_2SO_4$ , the result is:  
 136

$$k_1 \cdot [SA_{monomer}] \cdot [H_2SO_4] = CS \cdot [SA_{dimer}] + CS \cdot [SA_{trimer}] + \alpha \cdot [SA_{dimer}] \cdot N_{pos} + \alpha \cdot [SA_{trimer}] \cdot N_{pos}, \quad (7)$$

$$[H_2SO_4] = \frac{(CS + \alpha \cdot N_{pos}) \cdot ([SA_{dimer}] + [SA_{trimer}])}{k_1 \cdot [SA_{monomer}]} \quad (8)$$

137

138 Besides the steady-state assumption, it should be noted that in deriving eq. 8 monomers, dimers and trimers were  
139 assumed to have the same loss rate (CS) onto pre-existing aerosol particles. This causes an additional, yet minor,  
140 uncertainty in the estimated H<sub>2</sub>SO<sub>4</sub> concentrations, as such loss rates are dependent on the size/mass of the clusters  
141 (e.g. Lehtinen et al., 2007; Tuovinen et al., 2021). According to Tuovinen et al. (2021), the CS of H<sub>2</sub>SO<sub>4</sub> clusters  
142 decreases with increasing number of H<sub>2</sub>SO<sub>4</sub> molecules. The study shows that the CS of the SA<sub>dimer</sub> clustered with  
143 ammonia decreases to 68% (compared to one H<sub>2</sub>SO<sub>4</sub> molecule) and for SA<sub>pentamer</sub> with four ammonia molecules  
144 to 42%. However, the order of magnitude of the CS remains the same, and the effect on the estimation of the  
145 H<sub>2</sub>SO<sub>4</sub> concentration is assumed to be negligible. Additionally, the CS for ions is higher than for neutral  
146 compounds. The enhancement of CS has shown to reach a maximum value of 2 when the pre-existing particles  
147 are < 10 nm and decreases to 1 when the pre-existing particles are > 100 nm, as shown by Mahfouz and Donahue  
148 (2021). [The impact of ions on CS and estimated SA concentrations depends thereby on the environmental  
149 conditions determining the size distribution and charges of the pre-existing particle population. Neglecting the  
150 size-dependency of CS between the SA monomers, dimers and trimers causes additional errors in estimated SA  
151 concentrations; however, it is difficult to determine this effect in ambient measurements having limited data and  
152 instrumentation.](#)

153  
154 Furthermore, the derivation neglects the losses of SA<sub>trimer</sub> to the SA<sub>tetramer</sub> and larger clusters, as well as the  
155 clustering of sulfuric acid ion clusters with water and base molecules, such as NH<sub>3</sub>. Those simplifications can  
156 cause an underestimation of the H<sub>2</sub>SO<sub>4</sub> concentration with the presented method. If necessary, the method can  
157 easily be adapted, and bigger clusters can be included in the equation.

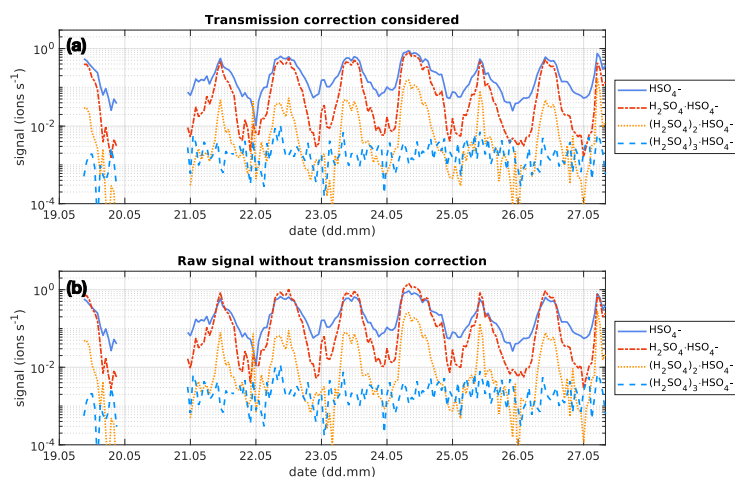
158  
159 From equation 8 we also see that the concentration of H<sub>2</sub>SO<sub>4</sub> is proportional to relative concentrations of sulfuric  
160 acid monomers, dimers and trimers clustered with the bisulphate ion:

$$[H_2SO_4] \sim \frac{[SA_{dimer}] + [SA_{trimer}]}{[SA_{monomer}]} \quad (9)$$

162  
163 To estimate the H<sub>2</sub>SO<sub>4</sub> concentration with the ion mode API-TOF, we can therefore use this theoretical approach,  
164 in particular Eq. 8. For the collision rate of H<sub>2</sub>SO<sub>4</sub> with HSO<sub>4</sub><sup>-</sup> we use  $k_1 = 2 \cdot 10^{-9} \text{ cm}^3 \text{ molecule}^{-1} \text{ s}^{-1}$  as in Lovejoy  
165 et al. (2004). The value of CS is calculated based on Kulmala et al. (2012). Even if the CS was unknown due, for  
166 example, to the lack of particle measurements, the daytime variability of the H<sub>2</sub>SO<sub>4</sub> concentration could still be  
167 estimated by using the relation of the H<sub>2</sub>SO<sub>4</sub>-containing cluster with HSO<sub>4</sub><sup>-</sup>, as it is proportional to the H<sub>2</sub>SO<sub>4</sub>  
168 concentration (see eq. 9). If the concentration of positive small ions is not available, it can be assumed to be in the  
169 range of 500 – 1000 cm<sup>-3</sup> which is a reasonable approximation for the average concentration (Hirsikko et al.,  
170 2011).

171  
172 As the transmission of clusters within an API-TOF depends on the tuning of the instrument and on the pressures  
173 within its chambers, the transmission efficiency needs to be considered, in order to get reliable concentrations of  
174 the SA<sub>monomer</sub>, SA<sub>dimer</sub>, and SA<sub>trimer</sub>. Fig. 1 shows the transmission efficiency curve of the API-TOF used at the  
175 SMEAR II station and Neumayer Station III. The effect of applying the transmission correction to the different

176 SA clusters is depicted in Fig. 3 for the time series at the SMEAR II station. All ion signals were normalised to a  
 177 transmission of 1%. As can be determined from Fig. 1a, the SA<sub>monomer</sub>'s transmission at SMEAR II was ~1%,  
 178 while the dimer and trimer were corrected by a factor of 1/1.8 and 1/1.65, respectively. The correction was also  
 179 applied on the ions measured at the Neumayer Station III according to the APi-TOF's transmission (Fig. 1b).  
 180



181  
 182 **Figure 3** Time series of the bisulphate ion ( $\text{HSO}_4^-$ , SA<sub>monomer</sub>),  $\text{H}_2\text{SO}_4$  clustered with bisulphate ( $\text{H}_2\text{SO}_4\cdot\text{HSO}_4^-$ , SA<sub>dimer</sub>), two  
 183  $\text{H}_2\text{SO}_4$  molecules clustered with the bisulphate ion ( $(\text{H}_2\text{SO}_4)_2\cdot\text{HSO}_4^-$ , SA<sub>trimer</sub>) and three  $\text{H}_2\text{SO}_4$  molecules clustered with the  
 184 bisulphate ion ( $(\text{H}_2\text{SO}_4)_3\cdot\text{HSO}_4^-$ , SA<sub>tetramer</sub>) between 19 and 27 May 2017 at SMEAR II station, Hyttiälä, Finland. The  
 185 concentration is given in ions  $\text{s}^{-1}$  as measured by the APi-TOF. The upper panel shows the concentration of the clusters  
 186 considering the transmission efficiency of the instrument (see Fig. 1). The lower panel shows the concentration of the clusters  
 187 without that correction and assuming a constant transmission efficiency of 1% for all ions.

188  
 189

### 190 3 Validation

191 We tested the expression derived above using a dataset collected during inter-comparison measurements at the  
 192 SMEAR II station in Hyttiälä, Finland (Hari and Kulmala, 2005). In Fig. 4 we show the time series of the observed  
 193  $\text{H}_2\text{SO}_4$  concentrations, measured with a CI-APi-TOF. The CI-APi-TOF was calibrated for sulfuric acid, based on  
 194 the method by Kürten et al., (2012) and resulted in a calibration factor of  $2.5 \times 10^9$ . Additionally, we show the  
 195 estimated sulfuric acid concentration based on APi-TOF measurements together with Eq. 8 and the sulfuric acid  
 196 proxy concentration (Dada et al., 2020). The concentration of positive ions for the estimated sulfuric acid  
 197 concentration was obtained from a Neutral cluster and Air Ion Spectrometer (NAIS, Airel Ltd., Mirme and Mirme,  
 198 2013).

199  
 200 The estimated  $\text{H}_2\text{SO}_4$  concentration agrees with the measured one during most of the daytime. Between 06:00 and  
 201 18:00 local time, the correlation ( $R^2$ ) between the estimated and measured  $\text{H}_2\text{SO}_4$  concentration is equal to 0.85

202 with a root mean square error (RMSE) of  $4.12 \times 10^5 \text{ cm}^{-3}$ . During night-time, the corresponding values are 0.85  
203 and  $3.23 \times 10^5 \text{ cm}^{-3}$  (Table 1).

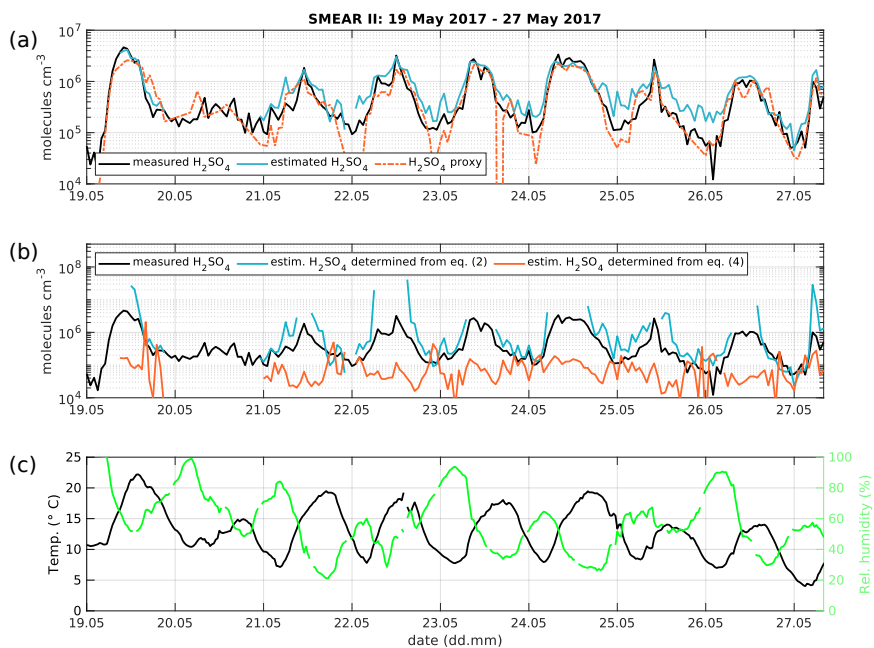
204  
205 The scatter plot in Fig. 5 shows that the estimated  $\text{H}_2\text{SO}_4$  concentrations agree well with the observed one when  
206  $\text{H}_2\text{SO}_4$  concentrations are larger than  $2 \times 10^6 \text{ cm}^{-3}$ , demonstrating that our method works particularly well at the  
207 SMEAR II station during conditions that favour the formation of  $\text{H}_2\text{SO}_4$ -containing clusters.

208  
209  
210 **Table 1:** Root mean square error (RMSE) and  $R^2$  of the estimated  $\text{H}_2\text{SO}_4$  concentration at the SMEAR II station and Neumayer  
211 Station III. The day- and night-time are split in 06:00 – 18:00 local time (LT) and 18:00 – 06:00 LT, respectively. For the  
212 SMEAR II station, we also show the RMSE and  $R^2$  of the  $\text{H}_2\text{SO}_4$  proxy calculated with the introduced method by (Dada et al.,  
213 2020).

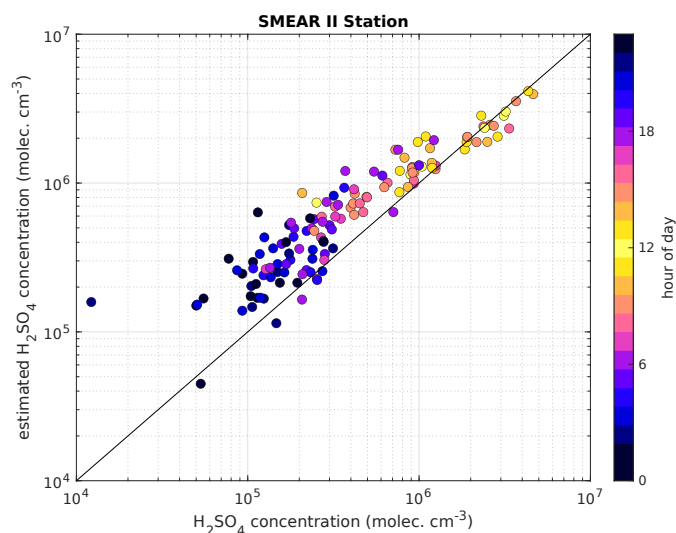
	Root mean square error (RMSE)		
	SMEAR II		Neumayer Station III
	Estimated $\text{H}_2\text{SO}_4$ eq. (8)	$\text{H}_2\text{SO}_4$ proxy	Estimated $\text{H}_2\text{SO}_4$ eq. (8)
Daytime	$4.12 \times 10^5 \text{ cm}^{-3}$	$5.54 \times 10^5 \text{ cm}^{-3}$	$1.43 \times 10^6 \text{ cm}^{-3}$
Night-time	$3.23 \times 10^5 \text{ cm}^{-3}$	$4.25 \times 10^5 \text{ cm}^{-3}$	$1.63 \times 10^6 \text{ cm}^{-3}$
$R^2$			
Daytime	0.85	0.78	0.48
Night-time	0.85	0.84	0.37

214  
215





216  
 217 **Figure 4** (a) Time series of measured H<sub>2</sub>SO<sub>4</sub> concentration from the CI-API-TOF (black) and estimated H<sub>2</sub>SO<sub>4</sub> concentration  
 218 from the API-TOF (blue) and H<sub>2</sub>SO<sub>4</sub> proxy from Dada et al. (2020) (orange) between 19 and 27 May 2017. The concentration  
 219 is given in molecules cm<sup>-3</sup>. (b) Measured H<sub>2</sub>SO<sub>4</sub> concentration as in panel (a) in black and determined concentration from eq.  
 220 2 (blue) and eq. 4 (orange). (c) Temperature and relative humidity.  
 221



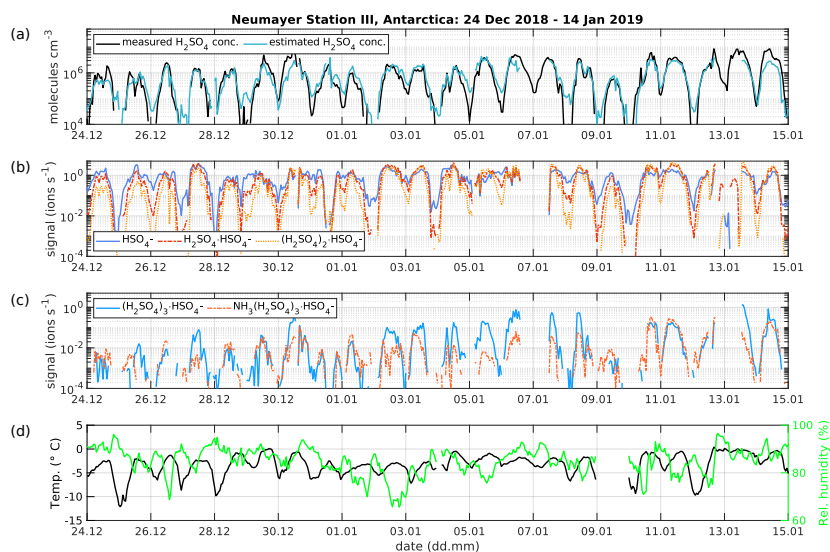
222  
 223 **Figure 5** Measured H<sub>2</sub>SO<sub>4</sub> concentration using a CI-API-TOF (horizontal-axis) versus estimated H<sub>2</sub>SO<sub>4</sub> concentration based  
 224 on API-TOF results (vertical-axis) at SMEAR II station. For the estimation of H<sub>2</sub>SO<sub>4</sub>, the transmission efficiency was taken  
 225 into account. The colour is indicating the hour of the day and the black line is the 1:1 ratio. Between 08:00 and 16:00 local  
 226 time, the concentrations are agreeing well. The shown data contains the time period from 19 to 27 May 2017. The overall  
 227 correlation coefficient (Pearson) is 0.94.

228  
 229 For the sake of completeness, the estimation of the H<sub>2</sub>SO<sub>4</sub> concentration determined from Eqs. 2 and 4, assuming  
 230 pseudo-steady state, are depicted in Fig. 4b. The estimated H<sub>2</sub>SO<sub>4</sub> concentration from Eq. 2 is overestimating,  
 231 while solving Eq. 4 for H<sub>2</sub>SO<sub>4</sub> is underestimating the real concentration as those equations are only  
 232 approximations. By combining the various approximations, Eq. 8 yields in the best fit to the observed SA  
 233 concentration.

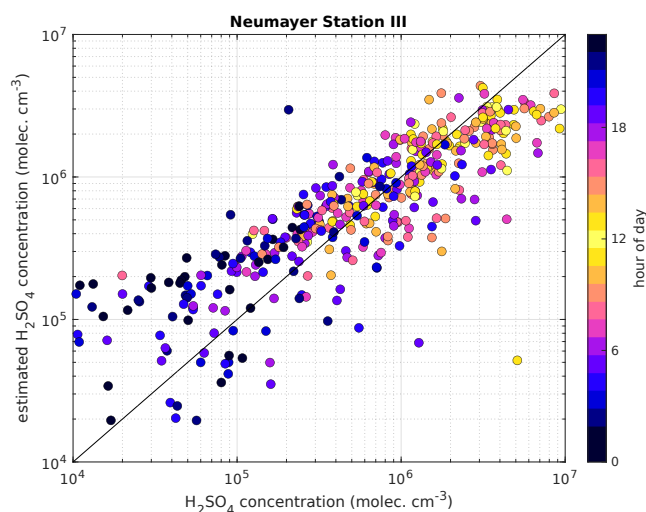
234  
 235 The presented method was also applied to measurements taken at the Neumayer Station III, Antarctica, in order  
 236 to test it in a different environment. Here, we used the condensation sink reported by Weller et al. (2015) at  
 237 Neumayer Station of  $1 \times 10^{-3} \text{ s}^{-1}$ . Figure 6 shows a three-week period between 24 December 2018 and 14 January  
 238 2019. The calibration factor of the CI-API-TOF used for measuring the sulfuric acid concentration is  $4.9 \times 10^9$ .  
 239 Here, the estimated sulfuric acid concentration underestimates the measured concentration when the SA<sub>tetramer</sub> and  
 240 NH<sub>3</sub>(H<sub>2</sub>SO<sub>4</sub>)<sub>3</sub>HSO<sub>4</sub>- cluster show high concentrations (Fig. 6c). A possible explanation for the underestimation  
 241 might be the neglect of the growth of sulfuric acid to oligomers larger than the tetramer, as well as its clustering  
 242 with bases and water (Fig. 6b and c). In coastal Antarctica, the main nucleating mechanism was observed to be  
 243 negative ion-induced sulfuric acid-ammonia nucleation, acting as a major sink for sulfuric acid molecules due to  
 244 its clustering with bases (Jokinen et al., 2018). Including the SA<sub>tetramer</sub> and SA<sub>tetramer</sub> clustered with NH<sub>3</sub> in the  
 245 estimation equation improved the correlation (R<sup>2</sup>) from 0.48 to 0.54. Furthermore, as mentioned above, the value  
 246 of CS for Neumayer was assumed to be constant ( $10^{-3} \text{ s}^{-1}$ ) due to the lack of data needed for its calculation. This

**Deleted:** The estimated H<sub>2</sub>SO<sub>4</sub> concentration from Eq. 2 is highly overestimating, since the losses of the SA<sub>dimer</sub> to the SA<sub>trimer</sub> are neglected. When solving Eq. 4 for H<sub>2</sub>SO<sub>4</sub>, only the needed H<sub>2</sub>SO<sub>4</sub> for the formation of the trimer is considered and the monomer and dimer production are neglected. Consequently, the resulting estimated H<sub>2</sub>SO<sub>4</sub> concentration is vastly underestimating the real concentration.

254 simplification certainly causes additional errors in estimated SA concentrations, especially during periods of high  
 255 sea salt concentrations causing potentially large variations in values of CS. Nevertheless, the diurnal variation of  
 256 the SA concentration is represented well by this method. During times with lower sulfuric acid concentrations,  
 257 our method gives higher values than the measured concentrations (Fig. 6).



258  
 259 **Figure 6** (a) Time series of measured  $\text{H}_2\text{SO}_4$  concentration from the CI-APi-TOF (black) and estimated  $\text{H}_2\text{SO}_4$  concentration  
 260 from the APi-TOF (blue) between 24 December 2018 and 14 January 2019 at Neumayer Station III, Antarctica. The  
 261 concentration is given in molecules  $\text{cm}^{-3}$ . (b) Time series of the bisulphate ion ( $\text{HSO}_4^-$ ,  $\text{SA}_{\text{monomer}}$ ),  $\text{H}_2\text{SO}_4$  clustered with  
 262 bisulphate ( $\text{H}_2\text{SO}_4\text{-HSO}_4^-$ ,  $\text{SA}_{\text{dimer}}$ ), two  $\text{H}_2\text{SO}_4$  molecules clustered with the bisulphate ion ( $(\text{H}_2\text{SO}_4)_2\text{-HSO}_4^-$ ,  $\text{SA}_{\text{trimer}}$ ) and (c)  
 263 three  $\text{H}_2\text{SO}_4$  molecules clustered with the bisulphate ion ( $(\text{H}_2\text{SO}_4)_3\text{-HSO}_4^-$ ,  $\text{SA}_{\text{tetramer}}$ ) as well as the  $\text{SA}_{\text{tetramer}}$  clustered with  
 264  $\text{NH}_3$ . (d) Temperature and relative humidity measured at Neumayer Station III.  
 265



266  
 267 **Figure 7** Measured  $\text{H}_2\text{SO}_4$  concentration using a CI-APi-TOF (horizontal axis) versus estimated  $\text{H}_2\text{SO}_4$  concentration based  
 268 on APi-TOF results (vertical axis) at the Neumayer Station III. For the estimation of  $\text{H}_2\text{SO}_4$ , the transmission efficiency was  
 269 taken into account. The colour is indicating the hour of the day and the black line is the 1:1 ratio. The shown data contains the  
 270 time period from 24 December 2016 to 14 January 2019. The overall correlation coefficient (Pearson) is 0.77.  
 271

272  
 273 **4 Conclusions**

274 Here we derived a theoretical expression to estimate  $\text{H}_2\text{SO}_4$  concentrations based on APi-TOF measurements of  
 275 ambient ions. The estimation agrees well with the measured concentration during daytime in the boreal forest ( $R^2$   
 276 = 0.85), indicating that the estimation is able to represent the diurnal variation and trend of  $\text{H}_2\text{SO}_4$  concentrations  
 277 during most of the time when active clustering of sulfuric acid is inducing the initial step(s) of atmospheric new  
 278 particle formation. However, in an atmosphere, where sulfuric acid is the dominating pathway for initiating new  
 279 particle formation, the method might underestimate the  $\text{H}_2\text{SO}_4$  concentrations, as this method does not include the  
 280 rapid clustering to bigger of sulfuric acid clusters and clustering with bases directly, e.g. in the Antarctic  
 281 atmosphere ( $R^2 = 0.48$ ; during daytime).  
 282

283 The APi-TOF's "ion mode", i.e. direct ion sampling without chemical ionisation, remains a crucial tool in many  
 284 field deployments and laboratory studies, since it is extremely sensitive and allows for observing atmospheric  
 285 clustering molecule by molecule, which in most cases is impossible when relying on chemical ionization.  
 286 Therefore, having available a reliable estimate of  $\text{H}_2\text{SO}_4$  concentration allows us to utilise the APi-TOF ion mode  
 287 even more effectively.  
 288

289  
 290 **Data availability**

291 The data can be accessed via Zenodo (10.5281/zenodo.5266313).

292

293 **Author contribution**

294 LJB, SS, VMK and MK designed the study. LJB and MS performed the measurements. SS and LJB derived the  
295 equations. LJB processed and analysed the data and performed the data visualisation. MK and VMK supervised  
296 the process. All authors commented and edited the paper.

297

298 **Competing interests**

299 The authors declare that they have no conflict of interest.

300

301 **Acknowledgements**

302 We acknowledge the following projects: ACCC Flagship funded by the Academy of Finland grant number  
303 337549, Academy professorship funded by the Academy of Finland (grant no. 302958), Academy of Finland  
304 projects no. 1325656, 310682, 316114, 325647 and 296628, Russian Mega Grant project “Megapolis - heat and  
305 pollution island: interdisciplinary hydroclimatic, geochemical and ecological analysis” application reference  
306 2020-220-08-5835, “Quantifying carbon sink, CarbonSink+ and their interaction with air quality” INAR project  
307 funded by Jane and Aatos Erkkö Foundation, European Research Council (ERC) project ATM-GTP Contract No.  
308 742206 and GASPARCON, grant agreement no. 714621. We thank the tofTools team for providing the tools for  
309 the mass spectrometry analysis. We thank the technical and scientific staff in Hyytiälä SMEAR II and the  
310 technicians and scientists of the Neumayer overwintering teams of the years 2018 and 2019. We thank Lubna  
311 Dada for calculating the SA proxy for SMEAR II station. We thank Janne Lampilahti for providing the codes to  
312 process the NAIS dataset.

313 **References**

- 314 Arnold, F. and Fabian, R.: First measurements of gas phase sulphuric acid in the stratosphere, 283, 55–57,  
315 <https://doi.org/10.1038/283055a0>, 1980.
- 316 Beck, L. J., Sarnela, N., Junninen, H., Hoppe, C. J. M., Garmash, O., Bianchi, F., Riva, M., Rose, C., Peräkylä,  
317 O., Wimmer, D., Kausiala, O., Jokinen, T., Ahonen, L., Mikkilä, J., Hakala, J., He, X.-C., Kontkanen, J., Wolf,  
318 K. K. E., Cappelletti, D., Mazzola, M., Traversi, R., Petroselli, C., Viola, A. P., Vitale, V., Lange, R., Massling,  
319 A., Nøjgaard, J. K., Krejci, R., Karlsson, L., Zieger, P., Jang, S., Lee, K., Vakkari, V., Lampilahti, J., Thakur, R.  
320 C., Leino, K., Kangasluoma, J., Duplissy, E.-M., Siivola, E., Marbouti, M., Tham, Y. J., Saiz-Lopez, A., Petäjä,  
321 T., Ehn, M., Worsnop, D. R., Skov, H., Kulmala, M., Kerminen, V.-M., and Sipilä, M.: Differing Mechanisms  
322 of New Particle Formation at Two Arctic Sites, *Geophysical Research Letters*, 48,  
323 <https://doi.org/10.1029/2020GL091334>, 2021.
- 324 Birmili, W., Berresheim, H., Plass-Dülmer, C., Elste, T., Gilge, S., Wiedensohler, A., and Uhrner, U.: The  
325 Hohenpeissenberg aerosol formation experiment (HAFEX): a long-term study including size-resolved aerosol,  
326 H<sub>2</sub>SO<sub>4</sub>, OH, and monoterpene measurements, 3, 361–376, <https://doi.org/10.5194/acp-3-361-2003>, 2003.
- 327 Cai, R., Yan, C., Yang, D., Yin, R., Lu, Y., Deng, C., Fu, Y., Ruan, J., Li, X., Kontkanen, J., Zhang, Q.,  
328 Kangasluoma, J., Ma, Y., Hao, J., Worsnop, D. R., Bianchi, F., Paasonen, P., Kerminen, V.-M., Liu, Y., Wang,  
329 L., Zheng, J., Kulmala, M., and Jiang, J.: Sulfuric acid–amine nucleation in urban Beijing, 21, 2457–2468,  
330 <https://doi.org/10.5194/acp-21-2457-2021>, 2021.
- 331 Dada, L., Ylivinkka, I., Baalbaki, R., Li, C., Guo, Y., Yan, C., Yao, L., Sarnela, N., Jokinen, T., Daellenbach, K.  
332 R., Yin, R., Deng, C., Chu, B., Nieminen, T., Wang, Y., Lin, Z., Thakur, R. C., Kontkanen, J., Stolzenburg, D.,  
333 Sipilä, M., Hussein, T., Paasonen, P., Bianchi, F., Salma, I., Weidinger, T., Pikridas, M., Sciare, J., Jiang, J.,  
334 Liu, Y., Petäjä, T., Kerminen, V.-M., and Kulmala, M.: Sources and sinks driving sulfuric acid concentrations in  
335 contrasting environments: implications on proxy calculations, 20, 11747–11766, [https://doi.org/10.5194/acp-20-](https://doi.org/10.5194/acp-20-11747-2020)  
336 11747-2020, 2020.
- 337 Ehn, M., Junninen, H., Petäjä, T., Kurtén, T., Kerminen, V.-M., Schobesberger, S., Manninen, H. E., Ortega, I.  
338 K., Vehkamäki, H., Kulmala, M., and Worsnop, D. R.: Composition and temporal behavior of ambient ions in  
339 the boreal forest, 10, 8513–8530, <https://doi.org/10.5194/acp-10-8513-2010>, 2010.
- 340 Eisele, F. L.: Natural and anthropogenic negative ions in the troposphere, 94, 2183–2196,  
341 <https://doi.org/10.1029/JD094iD02p02183>, 1989.
- 342 Hari, P. and Kulmala, M.: Station for Measuring Ecosystem–Atmosphere Relations (SMEAR II), *Bor. Env.*  
343 *Res.*, 10, 315–322, 2005.
- 344 Herrmann, W., Eichler, T., Bernardo, N., and Fernandez de la Mora, J.: Turbulent transition arises at Re 35 000  
345 in a short Vienna type DMA with a large laminarizing inlet, *Proceedings of the annual conference of the*  
346 *AAAR*, St. Louis, MO, 6–10 October 2000.
- 347  
348 Hirsikko, A., Nieminen, T., Gagné, S., Lehtipalo, K., Manninen, H. E., Ehn, M., Hörrak, U., Kerminen, V.-M.,  
349 Laakso, L., McMurry, P. H., Mirme, A., Mirme, S., Petäjä, T., Tammets, H., Vakkari, V., Vana, M., and  
350 Kulmala, M.: Atmospheric ions and nucleation: a review of observations, 11, 767–798,  
351 <https://doi.org/10.5194/acp-11-767-2011>, 2011.
- 352 Jokinen, T., Sipilä, M., Junninen, H., Ehn, M., Lönn, G., Hakala, J., Petäjä, T., Mauldin III, R. L., Kulmala, M.,  
353 and Worsnop, D. R.: Atmospheric sulphuric acid and neutral cluster measurements using CI-APi-TOF, 12,  
354 4117–4125, <https://doi.org/10.5194/acp-12-4117-2012>, 2012.
- 355 Jokinen, T., Sipilä, M., Kontkanen, J., Vakkari, V., Tisler, P., Duplissy, E.-M., Junninen, H., Kangasluoma, J.,  
356 Manninen, H. E., Petäjä, T., Kulmala, M., Worsnop, D. R., Kirkby, J., Virkkula, A., and Kerminen, V.-M.: Ion-  
357 induced sulfuric acid–ammonia nucleation drives particle formation in coastal Antarctica, *Sci Adv*, 4,  
358 <https://doi.org/10.1126/sciadv.aat9744>, 2018.

359 Junninen, H., Ehn, M., Petäjä, T., Luosujärvi, L., Kotiaho, T., Kostiaainen, R., Rohner, U., Gonin, M., Fuhrer, K.,  
360 Kulmala, M., and Worsnop, D. R.: A high-resolution mass spectrometer to measure atmospheric ion  
361 composition, 3, 1039–1053, <https://doi.org/10.5194/amt-3-1039-2010>, 2010.

362 Kerminen, V.-M., Petäjä, T., Manninen, H. E., Paasonen, P., Nieminen, T., Sipilä, M., Junninen, H., Ehn, M.,  
363 Gagné, S., Laakso, L., Riipinen, I., Vehkamäki, H., Kurten, T., Ortega, I. K., Dal Maso, M., Brus, D.,  
364 Hyvärinen, A., Lihavainen, H., Leppä, J., Lehtinen, K. E. J., Mirme, A., Mirme, S., Hörrak, U., Berndt, T.,  
365 Stratmann, F., Birmili, W., Wiedensohler, A., Metzger, A., Dommen, J., Baltensperger, U., Kiendler-Scharr, A.,  
366 Mentel, T. F., Wildt, J., Winkler, P. M., Wagner, P. E., Petzold, A., Minikin, A., Plass-Dülmer, C., Pöschl, U.,  
367 Laaksonen, A., and Kulmala, M.: Atmospheric nucleation: highlights of the EUCAARI project and future  
368 directions, 10, 10829–10848, <https://doi.org/10.5194/acp-10-10829-2010>, 2010.

369 Kontkanen, J., Lehtinen, K. E. J., Nieminen, T., Manninen, H. E., Lehtipalo, K., Kerminen, V.-M., and Kulmala,  
370 M.: Estimating the contribution of ion–ion recombination to sub-2 nm cluster concentrations from atmospheric  
371 measurements, 13, 11391–11401, <https://doi.org/10.5194/acp-13-11391-2013>, 2013.

372 Kuang, C., McMurry, P. H., McCormick, A. V., and Eisele, F. L.: Dependence of nucleation rates on sulfuric  
373 acid vapor concentration in diverse atmospheric locations, 113, <https://doi.org/10.1029/2007JD009253>, 2008.

374 Kulmala, M., Vehkamäki, H., Petäjä, T., Dal Maso, M., Lauri, A., Kerminen, V.-M., Birmili, W., and McMurry,  
375 P. H.: Formation and growth rates of ultrafine atmospheric particles: a review of observations, *Journal of*  
376 *Aerosol Science*, 35, 143–176, <https://doi.org/10.1016/j.jaerosci.2003.10.003>, 2004.

377 Kulmala, M., Petäjä, T., Nieminen, T., Sipilä, M., Manninen, H. E., Lehtipalo, K., Dal Maso, M., Aalto, P. P.,  
378 Junninen, H., Paasonen, P., Riipinen, I., Lehtinen, K. E. J., Laaksonen, A., and Kerminen, V.-M.: Measurement  
379 of the nucleation of atmospheric aerosol particles, 7, 1651–1667, <https://doi.org/10.1038/nprot.2012.091>, 2012.

380 Kulmala, M., Petäjä, T., Ehn, M., Thornton, J., Sipilä, M., Worsnop, D. R., and Kerminen, V.-M.: Chemistry of  
381 Atmospheric Nucleation: On the Recent Advances on Precursor Characterization and Atmospheric Cluster  
382 Composition in Connection with Atmospheric New Particle Formation, 65, 21–37,  
383 <https://doi.org/10.1146/annurev-physchem-040412-110014>, 2014.

384 Kürten, A., Rondo, L., Ehrhart, S., and Curtius, J.: Calibration of a Chemical Ionization Mass Spectrometer for  
385 the Measurement of Gaseous Sulfuric Acid, *J. Phys. Chem. A*, 116, 6375–6386,  
386 <https://doi.org/10.1021/jp212123n>, 2012.

387 Lehtinen, K. E. J., Dal Maso, M., Kulmala, M., and Kerminen, V.-M.: Estimating nucleation rates from apparent  
388 particle formation rates and vice versa: Revised formulation of the Kerminen–Kulmala equation, *Journal of*  
389 *Aerosol Science*, 38, 988–994, <https://doi.org/10.1016/j.jaerosci.2007.06.009>, 2007.

390 Lovejoy, E. R., Curtius, J., and Froyd, K. D.: Atmospheric ion-induced nucleation of sulfuric acid and water,  
391 109, <https://doi.org/10.1029/2003JD004460>, 2004.

392 Lu, Y., Yan, C., Fu, Y., Chen, Y., Liu, Y., Yang, G., Wang, Y., Bianchi, F., Chu, B., Zhou, Y., Yin, R.,  
393 Baalbaki, R., Garmash, O., Deng, C., Wang, W., Liu, Y., Petäjä, T., Kerminen, V.-M., Jiang, J., Kulmala, M.,  
394 and Wang, L.: A proxy for atmospheric daytime gaseous sulfuric acid concentration in urban Beijing, 19, 1971–  
395 1983, <https://doi.org/10.5194/acp-19-1971-2019>, 2019.

396 Mahfouz, N. G. A. and Donahue, N. M.: Technical note: The enhancement limit of coagulation scavenging of  
397 small charged particles, 21, 3827–3832, <https://doi.org/10.5194/acp-21-3827-2021>, 2021.

398 Mikkonen, S., Romakkaniemi, S., Smith, J. N., Korhonen, H., Petäjä, T., Plass-Duelmer, C., Boy, M., McMurry,  
399 P. H., Lehtinen, K. E. J., Joutsensaari, J., Hamed, A., Mauldin III, R. L., Birmili, W., Spindler, G., Arnold, F.,  
400 Kulmala, M., and Laaksonen, A.: A statistical proxy for sulphuric acid concentration, 11, 11319–11334,  
401 <https://doi.org/10.5194/acp-11-11319-2011>, 2011.

402 Mirme, S. and Mirme, A.: The mathematical principles and design of the NAIS – a spectrometer for the  
403 measurement of cluster ion and nanometer aerosol size distributions, 6, 1061–1071, <https://doi.org/10.5194/amt-6-1061-2013>, 2013.

404

405 Ortega, I. K., Olenius, T., Kupiainen-Määttä, O., Loukonen, V., Kurtén, T., and Vehkamäki, H.: Electrical  
406 charging changes the composition of sulfuric acid–ammonia/dimethylamine clusters, 14, 7995–8007,  
407 <https://doi.org/10.5194/acp-14-7995-2014>, 2014.

408 Petäjä, T., Mauldin, I. I. I., Kosciuch, E., McGrath, J., Nieminen, T., Paasonen, P., Boy, M., Adamov, A.,  
409 Kotiaho, T., and Kulmala, M.: Sulfuric acid and OH concentrations in a boreal forest site, 9, 7435–7448,  
410 <https://doi.org/10.5194/acp-9-7435-2009>, 2009.

411 Schobesberger, S., Junninen, H., Bianchi, F., Lönn, G., Ehn, M., Lehtipalo, K., Dommen, J., Ehrhart, S., Ortega,  
412 I. K., Franchin, A., Nieminen, T., Riccobono, F., Hutterli, M., Duplissy, J., Almeida, J., Amorim, A.,  
413 Breitenlechner, M., Downard, A. J., Dunne, E. M., Flagan, R. C., Kajos, M., Keskinen, H., Kirkby, J., Kupc, A.,  
414 Kürten, A., Kurtén, T., Laaksonen, A., Mathot, S., Onnela, A., Praplan, A. P., Rondo, L., Santos, F. D.,  
415 Schallhart, S., Schnitzhofer, R., Sipilä, M., Tomé, A., Tsagkogeorgas, G., Vehkamäki, H., Wimmer, D.,  
416 Baltensperger, U., Carslaw, K. S., Curtius, J., Hansel, A., Petäjä, T., Kulmala, M., Donahue, N. M., and  
417 Worsnop, D. R.: Molecular understanding of atmospheric particle formation from sulfuric acid and large  
418 oxidized organic molecules, PNAS, 110, 17223–17228, <https://doi.org/10.1073/pnas.1306973110>, 2013.

419 Tuovinen, S., Kontkanen, J., Cai, R., and Kulmala, M.: Condensation sink of atmospheric vapors: the effect of  
420 vapor properties and the resulting uncertainties, Environ. Sci.: Atmos., 1, 543–557,  
421 <https://doi.org/10.1039/D1EA00032B>, 2021.

422 Wang, Z. B., Hu, M., Yue, D. L., Zheng, J., Zhang, R. Y., Wiedensohler, A., Wu, Z. J., Nieminen, T., and Boy,  
423 M.: Evaluation on the role of sulfuric acid in the mechanisms of new particle formation for Beijing case, 11,  
424 12663–12671, <https://doi.org/10.5194/acp-11-12663-2011>, 2011.

425 Weber, R. J., McMurry, P. H., Eisele, F. L., and Tanner, D. J.: Measurement of Expected Nucleation Precursor  
426 Species and 3–500-nm Diameter Particles at Mauna Loa Observatory, Hawaii, 52, 2242–2257,  
427 [https://doi.org/10.1175/1520-0469\(1995\)052](https://doi.org/10.1175/1520-0469(1995)052), 1995.

428 Weber, R. J., Marti, J. J., McMurry, P. H., Eisele, F. L., Tanner, D. J., and Jefferson, A.: Measured Atmospheric  
429 New Particle Formation Rates: Implications for Nucleation Mechanisms, 151, 53–64,  
430 <https://doi.org/10.1080/00986449608936541>, 1996.

431 Weller, R., Schmidt, K., Teinilä, K., and Hillamo, R.: Natural new particle formation at the coastal Antarctic site  
432 Neumayer, 15, 11399–11410, <https://doi.org/10.5194/acp-15-11399-2015>, 2015.

433 Yao, L., Garmash, O., Bianchi, F., Zheng, J., Yan, C., Kontkanen, J., Junninen, H., Mazon, S. B., Ehn, M.,  
434 Paasonen, P., Sipilä, M., Wang, M., Wang, X., Xiao, S., Chen, H., Lu, Y., Zhang, B., Wang, D., Fu, Q., Geng,  
435 F., Li, L., Wang, H., Qiao, L., Yang, X., Chen, J., Kerminen, V.-M., Petäjä, T., Worsnop, D. R., Kulmala, M.,  
436 and Wang, L.: Atmospheric new particle formation from sulfuric acid and amines in a Chinese megacity, 361,  
437 278–281, <https://doi.org/10.1126/science.aao4839>, 2018.

438